Vol. 23, No. 2(2024) Bio24219
Revista Mexicana de Ingeniería Química

Biochar-packed biofilter for the treatment of gases produced by accumulated *Sargassum* waste

Biofiltro relleno con biocarbón para el tratamiento de gases producidos por residuos acumulados de sargazo

B. Escobar[1,2*], J. M. Baas-López[1], R. Tapia-Tussell[1], E. Olguín-Maciel[1]

[1]*Centro de Investigación Científica de Yucatán. Unidad de Energía Renovable. Carretera Sierra Papacal-Chuburná Puerto, Km 5. Sierra Papacal, Mérida, 97302, Yucatán, México.*

[2]*CONAHCyT-Centro de Investigación Científica de Yucatán. Unidad de Energía Renovable. Carretera Sierra Papacal-Chuburná Puerto, Km 5. Sierra Papacal, Mérida, 97302, Yucatán, México.*

Received: November 30, 2023; Accepted: February 16, 2024

Abstract

A biofilter was built from the production of biochar obtained from *Sargassum* spp. (SKPH) as an environmentally friendly option for its application in problems related to the generation of gases such as H_2S, CO_2, and CH_4 that emanate during the decomposition process of accumulated *Sargassum* waste. The *Sargassum* was treated with KOH to obtain an activated biochar, estimating a surface area of 1319 m^2 g^{-1} with an average pore size of 1.447 nm. This surface area value allows its use as a biofilter to control H_2S, CO_2, and CH_4 gases. The analysis of textural properties and structure of biochar were studied by XRD, FTIR, BET, and CHN-S techniques. The characterization results by X-ray diffraction and Raman spectroscopy showed a biochar with amorphous characteristics. In this study, the constructed biofilter was filled with SKPH biochar; this system was interconnected to the reactor containing *Sargassum* spp. (freshly collected from the beach) and to the portable gas meter. The results showed that sulfur, hydrogen, and nitrogen were significantly higher in the SKPH-LB sample. In general, biochar made it possible to demonstrate its efficient use to control H_2S and CO_2 produced by the disposal of *Sargassum* waste, becoming a novel strategy to improve the elimination of toxic gases and reduce greenhouse gas emissions.

Keywords: biochar; biofilter; H_2S; *Sargassum* spp., waste.

Resumen

Se construyó un biofiltro a partir de la producción de biocarbón obtenido del *Sargassum* spp. (SKPH) como una opción amigable con el medio ambiente para su aplicación en problemas relacionados con la generación de gases como el H_2S, CO_2 y CH_4 que son emanados durante el proceso de descomposición de los residuos acumulados de sargazo. El sargazo fue tratado con KOH para la obtención de un biocarbón activado, estimándose un área superficial de 1319 m^2 g^{-1}. Este valor de área superficial permite su uso como biofiltro para el control de los gases de H_2S, CO_2 y CH_4. Las técnicas XRD, FTIR, BET y CHN-S estudiaron las propiedades texturales y la estructura del biocarbón. Los resultados de la caracterización por XRD y espectroscopia Raman mostraron un biocarbón con características amorfas. En este estudio el biofiltro construido fue rellenado con el biocarbón SKPH, este sistema se interconectó al reactor que contenía *Sargassum* spp. y al medidor de gas portátil. Los resultados mostraron que el azufre, el hidrógeno y el nitrógeno fueron significativamente mayores en la muestra SKPH-LB. En general, el uso del biocarbón demostró su uso eficiente para controlar el H_2S y el CO_2 producidos por la descomposición de los desechos de sargazo, convirtiéndose en una novedosa estrategia para mejorar la eliminación de gases tóxicos y reducir las emisiones de gases invernadero.

Palabras clave: biocarbón, biofiltro, H_2S, *Sargassum* spp, residuo.

*Corresponding author. *E-mail*: bem08@hotmail.com;
https://doi.org/10.24275/rmiq/Bio24219
ISSN:1665-2738, *issn-e*: 2395-8472

1 Introduction

In recent years, various materials such as iron-oxide-based materials (Feng *et al*., 2020), zeolites (Rahmani *et al*., 2023), polymeric membranes (Casadei *et al*., 2020), and activated carbon (de Oliveira *et al*., 2020) have been used to remove sulfurous compounds through adsorption. Hydrogen sulfide (H_2S) is a colorless, extremely dangerous, corrosive, flammable gas heavier than air. It has a somewhat sweet and rotten egg-like odor and can be poisonous in high concentrations. At as low as 0.008 ppm, it causes an odor nuisance (Cox *et al*., 2002). H_2S emissions are commonly found in volcanic eruptions, sulfur springs, fumes from underwater fissures, swamps, bodies of standing water, crude oil, and as a result of the organic decomposition of biomass (Cao *et al*., 2023). Industries such as seafood processing, farming, leather markets, compost plants, and wastewater treatment (Olortiga-Asencios *et al*., 2022) plants also produce H_2S (Letelier-Gordo *et al*., 2020). A new factor contributing to the increase in H_2S production is the environmental problem caused by the decomposition of macroalgae in the Mexican Caribbean. *Sargassum* spp. has been arriving regularly since 2014, transforming the white sand and turquoise sea landscape into a picture of yellow and brown colors that is quite daunting for water and beach activities. This contingency has been recurrent, and between July and August 2015, an average of 9726 m^3 of seaweed accumulated per month per km of coastline was observed (van Tussenbroek *et al*., 2017). This situation has led to various problems for the Quintana Roo coast in tourism, social, and environmental aspects. In the latter, the decrease in oxygen content, reduction in light, water quality degradation, beach erosion, etc. have caused mortality of near-shore seagrasses and fauna. *Sargassum* also affects daily life as rotten *Sargassum* produces H_2S when breathed in, and depending on the exposure time and concentration, it can cause serious health problems (Yaw Atiglo *et al*., 2024).

High concentrations of H_2S in sediment have been linked to mortality events in seagrass (Koch *et al*., 2022). H_2S is also responsible for serious environmental problems, such as acid precipitation and global warming. Other toxic compounds, such as carbon dioxide (CO_2) and methane (CH_4), which are part of greenhouse effect gases (GHG), can be stored in activated biochars that work as adsorbent materials (Gutiérrez-Bonilla *et al*., 2022). Currently, biofilters have become a popular substitute for traditional air treatment procedures, including odor control and the removal of volatile organic compounds (VOC) (Permana *et al*., 2022), as well as H_2S emissions. Biofilters are devices that transport a moist contaminated fluid through a permeable filled area (Danila *et al*., 2022). The effectiveness of biochar in a biofilter depends on numerous factors, including suitable packing materials, large surface area, specific surface area, pore volume, pore size distribution, good ion exchange capacity, high gas retention capacity, and improved selectivity (Das *et al*., 2019). Recent research has shown that biochar can be beneficial when included as an adsorbent in biofilters (Yang *et al*., 2023). Furthermore, biochar can be used alone or mixed with other substances as a filter medium in bioretention systems, water treatment, decontamination of urban stormwater, adsorption, etc. In research adsorption of CH_4, H_2S, and CO_2, it was determined that the physicochemical properties of biochars were related to the adsorption performance (Sethupathi *et al*., 2017). Adsorption has also been widely used for removing H_2S, using traditionally mesoporous materials with a larger surface area, which might enhance the adsorption potential (Izhar *et al*., 2022).

Biochar, a porous carbon-rich material produced from biomass under oxygen-limited conditions, is now being developed as an efficient adsorbent that has been widely used for vapor analysis, including the adsorption of H_2S (Han *et al*., 2020), CO_2, and CH_4. Moreover, biochar has a competitive advantage due to its low cost and can be obtained from any source of biomass. In recent years, various studies have been carried out that relate the type of biomass, the pyrolysis temperature, and the activation conditions using different atmospheres, and how these parameters affect the performance of biochar as CO_2 and H_2S adsorbent materials, finding important differences in its behavior with each of these gases, related to both the porous structure and the surface chemistry. Several authors consider that H and S are stored in the pores of the biochar without being chemically linked to the biocarbon. That is, it can be assumed that H_2S adsorbs on active sites of the biochar, that is to say, the surface chemistry of biochar could be altered to anchorage specific functional groups to selectively H_2S adsorption (Elsayed *et al*., 2009). A possible reaction mechanism during the H_2S adsorption onto biochar can be very complex with a diversity of sulfur products. Commonly, the reaction mechanics includes two steps: (1) physical adsorption in the presence of water, H_2S is adsorbed on the carbon surface, dissolved in water, and dissociated in an adsorbed state; (2) oxidation step. The adsorbed H_2S reacts with oxygen (O_2) to form ending products of elemental sulfur (S0), sulfur dioxide (SO_2), and sulfate (SO_4^{2-}) (Huang *et al*., 2022).

This study aims to present the findings of an experiment conducted in a laboratory using a biofilter that contained biochar SKPH. The biochar SKPH was derived from the remnants of *Sargassum* spp. and was

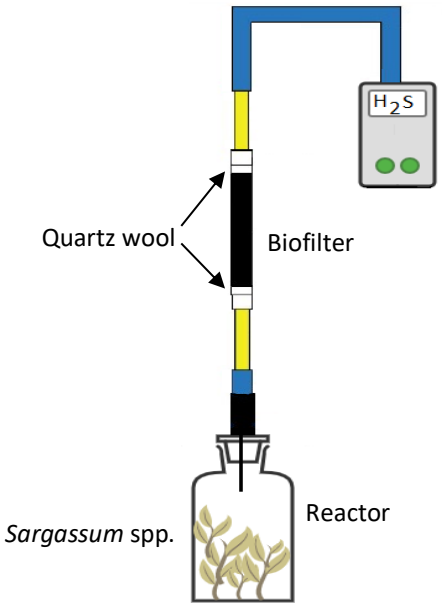

Figure 1 Diagram of the connection between the reactor and the biofilter.

used to eliminate greenhouse gases such as H_2S, CO_2, and CH_4. We analyzed the physicochemical properties and adsorption capacities of the SKPH sample before and after it was connected to the reactor.

2 Materials and methods

2.1 Biofilter

In this study, biochar was produced from *Sargassum* spp. (sample SKPH) according to reported in previous work (Pérez-Salcedo *et al*., 2019). The resulting biochar has an average pore size of approximately 1.4 nm and a measured surface area of around 1319 m^2 g^{-1}. A biofilter was then constructed by filling a transparent glass tube (10 mm diameter, 125 mm height) with 400 mg of the SKPH biochar, and sealing both ends with 100 g of quartz wool. Silicone hose reducers (9 mm diameter, 15 mm height) were connected to both sealed ends, and a plastic tube (8 mm diameter, 60 mm long) was attached. This system was then connected to six reactors containing 10 g fresh weight (without any prior treatment), which were placed in 250 mL serological bottles that were sealed with a tert-butyl plug and secured with a metal ring. The bottles were then incubated at 35 °C for natural decomposition, with headspace gas samples taken individually every 48 hours for 16 days. CO_2 and H_2S were measured using a Geotech 5000 gas analyzer portable equipment with three control units directly connected to the portable gas meter, and the other three reactors connected to the biofilter for 60 seconds. Figure 1 depicts the connection between the reactor, the sample of *Sargassum* spp, the biofilter, and the gas analyzer. SKPH-LB corresponds to the biochar sample that has been in contact with the gases generated by the decomposition of the biomass, that is to say, post-biofilter placement.

2.2 Characterization

Gas flow rates were measured and controlled using a Geotech Biogas 5000 gas analyzer in units of L min^{-1}. The total pore volume, specific surface area, and pore size distributions were determined through N2 physisorption tests using a Quantachrome Nova 2200e. The CHNS composition of biochars was examined using an automatic elemental analyzer, Thermoscientific Flash 2000. X-ray diffraction (XRD) patterns were obtained using Bruker D-2 Phaser with Cu-Kα radiation from 10° to 80°. The optimal preparation condition was achieved in all the characterizations.

3 Results and discussion

3.1 Physical and chemical characteristics of biochar

3.1.1 BET analysis

The biochar samples were degassed at 250 °C under vacuum for 5 hours to eliminate any impurities on their surface. The micropore BET assistant, which is included in the Novawin software, was employed to calculate the specific area (S_{BET}) and the Brunauer-Emmett-Teller (BET) equation using relative pressures ranging from 0.05 to 0.3 P/P0. The pore volume and diameter of the biochar were determined using the Barrett-Joyner-Halenda (BJH) method. The estimation was based on the quantity of gas adsorbed at a relative pressure close to unity (0.98 P/P_0). The pore size distribution graph was obtained through the novel Quenched Solid Density Functional Theory (QSDFT) method (Neimark *et al*., 2009). Figure 2(a) displays the adsorption and desorption isotherms of the SKPH and SKPH-LB samples before and after being connected to the reactor containing *Sargassum* waste. The data revealed an II-type isotherm with an H_4 hysteresis loop for both SKPH and SKPH-LB, suggesting that these biochar samples consist of micro-mesoporous adsorbent materials (Bedin *et al*., 2016). The pore structure parameters of biochar are a crucial factor that affects their adsorption properties. Figure 2(b) shows the pore size distribution of the biochars SKPH and SKPH-LB. Both samples show an undefined peak at around 1.4 nm which is attributed to the presence of micropores.

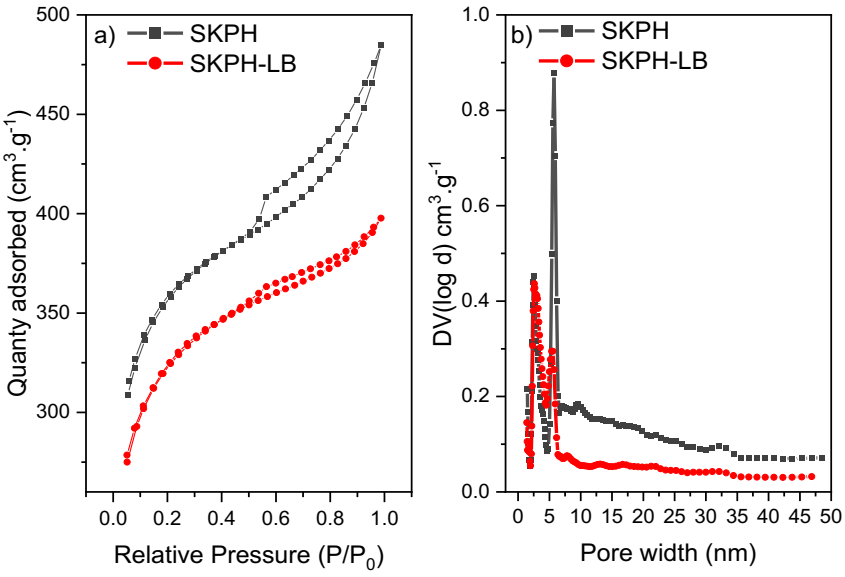

Figure 2 (a) Nitrogen adsorption-desorption isotherm of the samples SKPH and SKPH-LB, and (b) pore distribution.

Table 1 Pore structure parameters of the biochar samples.

Sample	BET surface area (m^2 g^{-1})	Average pore size (nm)	Pore volume (cm^3 g^{-1})
SKPH	1319	1.47	0.75
SKPH-LB	1191	1.41	0.61

Additionally, two increases in pore diameters can be seen at approximately 2.4 nm and 5.7 nm. These are associated with the formation of mesopores due to the activation process with KOH.

Table 1 provides a comparison of the average pore size, pore volume, and BET surface area for different biochar samples. The data in the table shows that the SKPH sample had a surface area of 1319 m^2 g^{-1}, while the SKPH-LB sample had a reduced surface area of 1191 m^2 g^{-1}. The reduction in surface area in the SKPH-LB sample could be due to the adsorption of nitrogen and sulfur trapped within the pores during the H_2S gas adsorption process, as revealed in the CHNS elemental analysis. This indicates that the micropores played a crucial role in the adsorption of H_2S. Furthermore, the pore diameter decreased slightly in the range of 5-5.6 nm, and according to the IUPAC classification, the biochar can be categorized as microporous. The adsorbed volume also decreased slightly in the 5-5.6 nm range, and to a lesser extent in the 1.40 to 1.50 nm range, indicating that both micropores and mesopores played a vital role in the H_2S, CO_2, and CH_4 adsorption process.

3.1.2 Elemental analysis CHN-S

The results of the elemental analysis of biochars are presented in Figure 3. The data shows that both samples, SKPH and SKPH-LB, have similar carbon contents, which are 74.42% and 76.37%, respectively. However, the sample SKPH-LB exhibits significantly

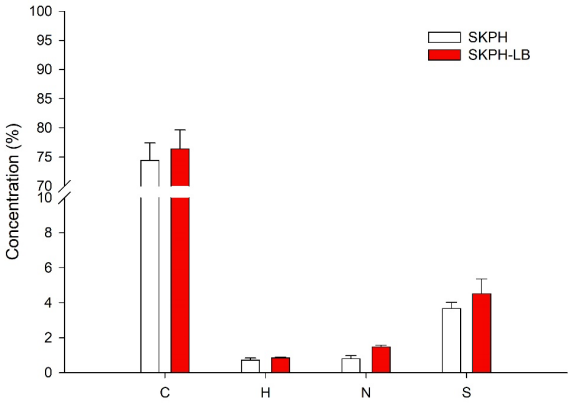

Figure 3 CHN-S analysis of the biochar SKPH and SKPH-LB.

higher concentrations of sulfur, hydrogen, and nitrogen. The sulfur concentration in SKPH-LB is 1.2 times higher than SKPH, while the hydrogen and nitrogen concentrations are 2.0 and 4.5 times higher, respectively. These increments represent increases of 107%, 355%, and 23%, respectively, compared to SKPH. Moreover, the increase in the amount of H, N, and S, in SKPH-LB suggests the retention of gases of H_2S and CH_4 produced by the reactor containing *Sargassum* waste, thereby decreasing the accessible surface area (1191 m^2 g^{-1}). One of the outstanding attributes of biochar that may contribute to the biofilter performance is its ability to adsorb gases and this characteristic is related to the high surface area (Thompson *et al.*, 2020). Furthermore, the results indicate that carbon is the primary component of biochar. The C, H, N, and S composition analysis of biochar is summarized in Table 2.

Table 2 CHNS elemental analyses of biochar in weight percentage.

Biochar	C	H	N	S
SKPH	74.42	0.71	0.80	3.67
SKPH-LB	76.37	0.84	1.47	4.52

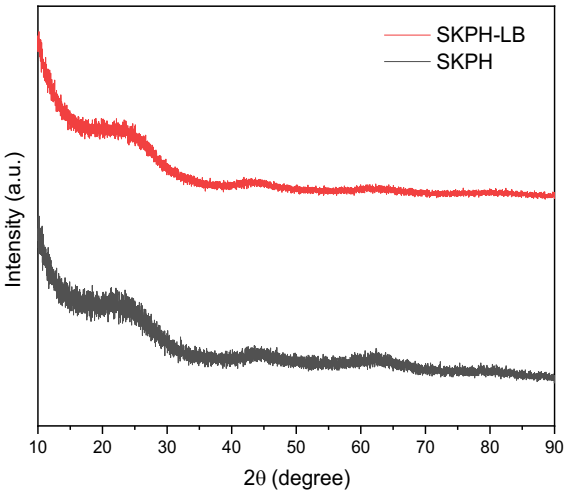

Figure 4 X-ray diffraction (XRD) patterns of SKPH and SKPH-LB.

3.1.3 X-ray powder diffraction (XRD)

In Figure 4, we can observe the amorphous carbon structures C (002) and C (100) for SKPH and SKPH-LB samples. The broad reflection between 20° and 25° indicates poor crystallinity without long-term crystalline order, in both samples, corresponding to the (002) plane of an ordered hexagonal graphitic carbon lattice. The peak located at 44.3° is associated with the plane (100), suggesting a more graphitic behavior (Wang *et al*., 2020). For both samples, the diffractograms of the biochars are very similar and these confirm that it contained mainly the amorphous compounds due to the decomposition of biomass indicating an amorphous carbon structure, presence of C, and graphite with randomly oriented aromatic carbon sheets. It is worth mentioning that the crystalline nature of biochar is the key to its stability, and this property largely depends on the biomass source and carbon content. The presence of amorphous carbon is associated with random mixtures of thermally variable molecules, aromatic polycondensates, poorly structured graphene stacks anchored in the amorphous phase, and turbostratic materials composed of chaotic graphite crystallites (Tomczyk *et al*., 2020).

3.1.4 Raman spectroscopy

Raman spectroscopy has been widely used to examine the carbon structure of both samples, pre (SKPH) and post-biofilter placement (SKPH-LB). In Figure 5, two peaks were observed at approximately 1322 and 1590 cm^{-1}, corresponding to the D-band and G-band. The D-peak was attributed to sp^3-hybridized carbon defects, while the G-peak represented the vibrations of sp^2-hybridized graphitic carbon in a two-dimensional hexagonal lattice (Sun *et al*., 2014). The results show a D and G peaks were very pronounced in both samples, and no significant differences were observed. It is possible to further analyze the diversity of defect degrees using the value of I_D/I_G. The ratio of the D peak and G peak's relative intensity (I_D/I_G) indicated the structural defects and disorders in the biochars. The biochar SKPH-LB had a higher degree of disorderliness in the carbon structure, with I_D/I_G = 1.41 ± 0.05, compared to sample SKPH, with I_D/I_G = 1.31 ± 0.01. The increase in the defect degree of this biochar could be attributed to the introduction of N and S in the biochar, according to the results of the CHN-S elemental analysis.

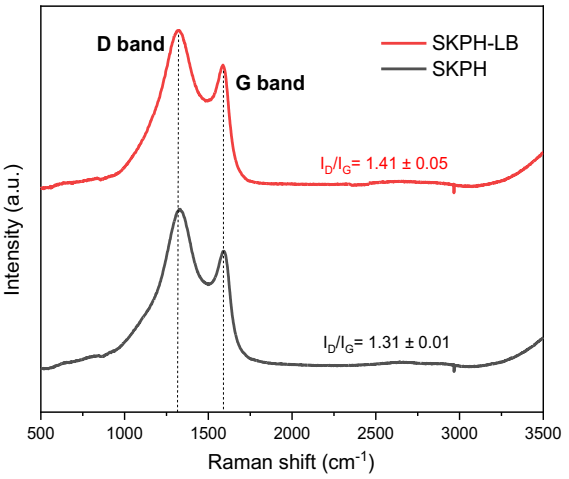

Figure 5. Raman spectra of the biochar SKPH and SKPH-LB.

3.2 Performance during the test

In Figure 6 (a) the line, indicated by black circles, shows the average values obtained from the direct H_2S emissions of the control group (SKPH). A concentration of 2,000 ppm was recorded during the first four days of sampling, and it reached the maximum value on day 10, with an average of 2,703 ppm. The lower line, indicated by empty circles, shows the average values obtained from the SKPH-LB sample passed through the biofilter. In SKPH-LB samples the maximum H_2S concentration was 120 ppm. This represents a greater than 95% decrease in the H_2S concentration concerning the control group emissions, which shows the efficiency of SKPH *Sargassum* biochar in removing this gas. In the literature there are other examples of the use of biochar, for example, biochar prepared from invasive algae *Sargassum* spp. was successfully employed as a sorbent for caffeine removal from water (Francoeur *et al*., 2021).

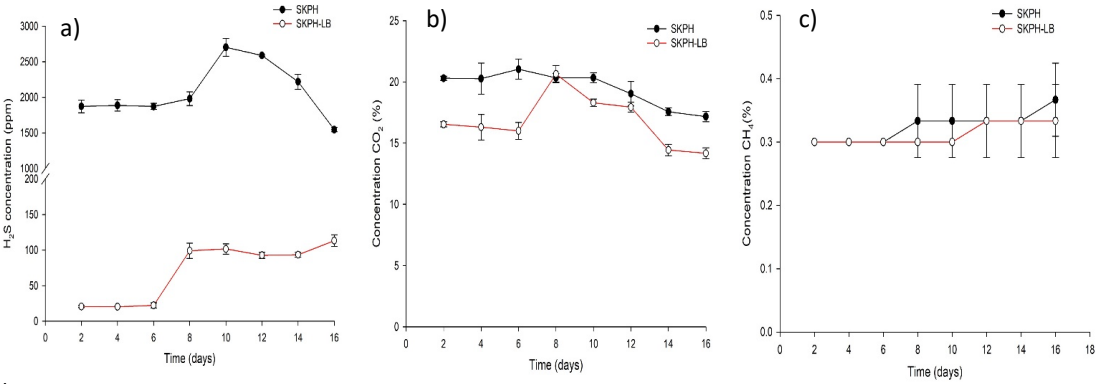

Figure 6 (a) Concentration of gases (a) H_2S, (b) CO_2, and (c) CH_4.

In this same sense, Truong *et al*., (2023) mentions the potential of biochar obtained from *Sargassum hemiphylum* to remove Cu(II) from aqueous solutions, leading to its high degree of applicability for water treatment. In addition, studies on *Sargassum* and *Enteromorpha* biochars indicate a high adsorption capacity which means good development potential in the field of H_2S removal (Han *et al*., 2020).

Figure 6 (b) shows the production of CO_2, and as in the case of H_2S, the values obtained from the direct measurement of the SKPH group are higher than those of the SKPH-LB sample. This suggests that biochar has the potential to absorb a significant portion of the CO_2 molecule (Zhang *et al*., 2022). In Figure 6 (c), the detected methane concentrations were very low, with the highest concentration being only 0.36%. This low level of methane emission can be attributed to the fact that the *Sargassum* used in this experiment was recently collected and in this type of sample, mainly sulfate-reducing bacteria have been identified, which favors the production of H_2S over methane (Hervé *et al*., 2021). Furthermore, some authors have suggested that the high sulfur content in algae negatively affects methane production (Maneein *et al*., 2021).

Conclusions

An inexpensive and straightforward biofilter was tested for removing H_2S, CO_2, and CH_4 using accumulated *Sargassum* waste. The results showed that the biofilter made with biochar from *Sargassum* spp. can significantly absorb H_2S and CO_2 gases. The nitrogen and sulfur content in the biochar increased after being exposed to reactor gases. To understand the physicochemical properties of the biochars, they were characterized by DRX, BET, and Raman analyses. The BET analysis revealed that the biochar's surface area decreased slightly after the H_2S gas adsorption process, reaching a minimum value of 1208 m^2 g^{-1} for sample SKPH-LB. This study opens an opportunity avenue for *Sargassum* waste, through the use of biochar. Therefore, we consider biochar as an important candidate for further research in the emissions control of toxic gases.

Acknowledgements

The authors would like to thank Mayli Carvajal Caamal and Laura Yaqueline Gómez Medina for their dedicated assistance in the laboratory.

References

Bedin, K.C., Martins, A.C., Cazetta, A.L., Pezoti, O., and Almeida, V.C. (2016). KOH-activated carbon prepared from sucrose spherical carbon: Adsorption equilibrium, kinetic and thermodynamic studies for Methylene Blue removal. *Chemical Engineering Journal 286*, 476-484. https://doi.org/10.1016/j.cej.2015.10.099

Cao, T., Zheng, Y., and Dong, H. (2023). Control of odor emissions from livestock farms: A review. *Environmental Research 225*, 115545. https://doi.org/10.1016/j.envres.2023.115545

Casadei, R., Baschetti, M.G., Yoo, M.J., Park, H.B., and Giorgini, L. (2020). Pebax® 2533/graphene oxide nanocomposite membranes for carbon capture. *Membranes 10*, 188. https://doi.org/10.3390/membranes10080188

Cox, H.H.J., and Deshusses, M.A. (2002). Co-treatment of H_2S and toluene in a biotrickling filter. *Chemical Engineering Journal 87*, 101-110. https://doi.org/10.1016/S1385-8947(01)00222-4

Danila, V., Zagorskis, A., and Januševičius, T. (2022). Effects of water content and irrigation of packing materials on the performance of

biofilters and biotrickling filters: A Review. *Processes 10*, 1304. https://doi.org/10.3390/pr10071304

Das, J., Rene, E.R., Dupont, C., Dufourny, A., Blin, J., and van Hullebusch, E.D. (2019). Performance of a compost and biochar packed biofilter for gas-phase hydrogen sulfide removal. *Bioresource Technology 273*, 581-591. https://doi.org/10.1016/j.biortech.2018.11.052

de Oliveira, J.L.B., Nascimento, B.O., Gonçalves, D.V., Santiago, R.G., Lucena, S.M.P. de Azevedo, D.C.S. and Bastos-Neto, M. (2020). Effect of ultramicropores on the mechanisms of H_2S retention from biogas. *Chemical Engineering Research and Design 154*, 241-249. https://doi.org/10.1016/j.cherd.2019.12.019

Elsayed, Y., Seredych, M., Dallas, A., and Bandosz, T.J. (2009). Desulfurization of air at high and low H_2S concentrations. *Chemical Engineering Journal 155*, 594-602. https://doi.org/10.1016/j.cej.2009.08.010

Feng, Y., Lu, J., Wang, J., Mi, J., Zhang, M., Ge, M., Li, Y., Zhang, Z., and Wang, W. (2020). Desulfurization sorbents for green and clean coal utilization and downstream toxics reduction: A review and perspectives. *Journal of Cleaner Production 273*, 123080. https://doi.org/10.1016/j.jclepro.2020.123080

Francoeur, M., Ferino-Pérez, A., Yacou, C., Jean-Marius, C., Emmanuel, E., Chérémond, Y., Jauregui-Haza, U., and Gaspard, S. (2021). Activated carbon synthetized from *Sargassum* (sp) for adsorption of caffeine: Understanding the adsorption mechanism using molecular modeling. *Journal of Environmental Chemical Engineering 9*, 104795. https://doi.org/10.1016/j.jece.2020.104795

Gutiérrez-Bonilla, E., Granados-Correa, F., Roa-Morales, G., and Balderas-Hernández, P. (2022). CO_2 capture on an optimally prepared highly microporous KOH-activated carbon from rice husk. *Revista Mexicana de Ingeniería Química 21*. https://doi.org/10.24275/rmiq/Mat2528

Han, X., Chen, H., Liu, Y., and Pan, J. (2020). Study on removal of gaseous hydrogen sulfide based on macroalgae biochars. *Journal of Natural Gas Science and Engineering 73*, 103068. https://doi.org/10.1016/j.jngse.2019.103068

Hervé, V., Lambourdière, J., René-Trouillefou, M., Devault, D.A., and Lopez, P.J. (2021). *Sargassum* differentially shapes the microbiota composition and diversity at coastal tide sites and inland storage sites on Caribbean islands. *Frontiers in Microbiology 12*, 701155. https://doi.org/10.3389/fmicb.2021.701155

Huang, D., Wang, N., Bai, X., Chen, Y., and Xu, Q. (2022). The influencing mechanism of O_2, H_2O, and CO_2 on the H_2S removal of food waste digestate-derived biochar with abundant minerals. *Biochar 4*, 71. https://doi.org/10.1007/s42773-022-00199-2

Izhar, T.N.T., Kee, G.Z., Saad, F.N.M., Rahim, S.Z.A., Zakarya, I.A., Besom, M.R.C., Ibad, M., and Syafiuddin, A. (2022). Adsorption of hydrogen sulfide (H_2S) from municipal solid waste by using biochars. *Biointerface Research in Applied Chemistry 12*, 8057-8069. https://doi.org/10.33263/BRIAC126.80578069

Koch, M. S., Johnson, C. R., Madden, C. J., and Pedersen, O. (2022). Low irradiance disrupts the internal O_2 dynamics of seagrass (*Thalassia testudinum*) leading to shoot meristem H_2S intrusion. *Aquatic Botany 181*, 103532. https://doi.org/10.1016/j.aquabot.2022.103532

Letelier-Gordo, C.O., Aalto, S.L., Suurnäkki, S., and Pedersen, P.B. (2020). Increased sulfate availability in saline water promotes hydrogen sulfide production in fish organic waste. *Aquacultural Engineering 89*, 102062. https://doi.org/10.1016/j.aquaeng.2020.102062

Maneein, S., Milledge, J.J., Harvey, P.J., and Nielsen, B.V. (2021). Methane production from *Sargassum* muticum: effects of seasonality and of freshwater washes. *Energy and Built Environment 2*, 235-242. https://doi.org/10.1016/j.enbenv.2020.06.011

Neimark, A.V., Lin, Y., Ravikovitch, P.I., and Thommes, M. (2009). Quenched solid density functional theory and pore size analysis of micro-mesoporous carbons. *Carbon 47*, 1617-1628. https://doi.org/10.1016/j.carbon.2009.01.050

Olortiga-Asencios, Y., Malvestio, L., Perpetuo, E., and Rotta, A. (2022). Characterization of seaweeds collected from Baixada Santista litoral, and their potentialuses as biosorbents of heavy metal cations. *Revista Mexicana de Ingeniería Química 21*, 2600. https://doi.org/10.24275/rmiq/IA2600

Pérez-Salcedo, K.Y., Alonso-Lemus, I.L., Quintana, P., Mena-Durán, C.J., Barbosa, R., and Escobar, B. (2019). Self-doped *Sargassum* spp. derived biocarbon as electrocatalysts for ORR in alkaline media. *International Journal of Hydrogen Energy 44*, 12399-12408. https://doi.org/https://doi.org/10.1016/j.ijhydene.2018.10.073

Permana, B.H., Thiravetyan, P., and Treesubsuntorn, C. (2022). Effect of airflow pattern and distance on removal of particulate matters and volatile organic compounds from cigarette smoke using *Sansevieria trifasciata* botanical biofilter. *Chemosphere 295*, 133919. https://doi.org/10.1016/j.chemosphere.2022.133919

Rahmani, M., Mokhtarani, B., and Rahmanian, N. (2023). High pressure adsorption of hydrogen sulfide and regeneration ability of ultra-stable Y zeolite for natural gas sweetening. *Fuel 343*, 127937. https://doi.org/10.1016/j.fuel.2023.127937

Sethupathi, S., Zhang, M., Rajapaksha, A.U., Lee, S.R., Nor, N.M., Mohamed, A.R., Al-Wabel, M., Lee, S.S., and Ok, Y.S. (2017). Biochars as potential adsorbers of CH_4, CO_2 and H_2S. *Sustainability (Switzerland) 9*, 121. https://doi.org/10.3390/su9010121

Sun, L., Fu, Y., Tian, C., Yang, Y., Wang, L., Yin, J., Ma, J., Wang, R., and Fu, H. (2014). Isolated boron and nitrogen sites on porous graphitic carbon synthesized from nitrogen-containing chitosan for supercapacitors. *ChemSusChem 7*, 1637-1645. https://doi.org/10.1002/cssc.201400048

Thompson, T.M., Young, B.R., and Baroutian, S. (2020). Efficiency of hydrothermal pretreatment on the anaerobic digestion of pelagic *Sargassum* for biogas and fertiliser recovery. *Fuel 279*, 118527. https://doi.org/10.1016/j.fuel.2020.118527

Tomczyk, A., Sokołowska, Z., and Boguta, P. (2020). Biochar physicochemical properties: pyrolysis temperature and feedstock kind effects. *Reviews in Environmental Science and Biotechnology 19*, 191-215. https://doi.org/10.1007/s11157-020-09523-3

Truong, Q.M., Nguyen, T.B., Chen, W.H., Chen, C.W., Patel, A.K., Bui, X.T., Singhania, R.R., and Dong, C.Di. (2023). Removal of heavy metals from aqueous solutions by high performance capacitive deionization process using biochar derived from *Sargassum hemiphyllum*. *Bioresource Technology 370*, 128524. https://doi.org/10.1016/j.biortech.2022.128524

van Tussenbroek, B.I., Hernández-Arana, H.A., Rodríguez-Martínez, R.E., Espinoza-Avalos, J., Canizales-Flores, H.M., González-Godoy, C.E., Barba-Santos, M.G., Vega-Zepeda, A., and Collado-Vides, L. (2017). Severe impacts of brown tides caused by *Sargassum* spp. on near-shore Caribbean seagrass communities. *Marine Pollution Bulletin 122*, 272-281. https://doi.org/10.1016/j.marpolbul.2017.06.057

Wang, X., Qi, L., and Wang, H. (2020). Carbon nanobeads collected from candle soot as an anode material with a highly pseudocapacitive Na^+ storage capability for dual-ion batteries. *Ionics 26*, 4533-4542. https://doi.org/10.1007/s11581-020-03630-5

Yang, Y., Kong, Z., Ma, H., Shao, Z., Wang, X., Shen, Y., and Chai, H. (2023). Insights into the transport and bio-degradation of dissolved inorganic nitrogen in the biochar-pyrite amended stormwater biofilter using dynamic modeling. *Journal of Environmental Management 347*, 119152. https://doi.org/10.1016/j.jenvman.2023.119152

Yaw Atiglo, D., Jayson-Quashigah, P.N., Sowah, W., Tompkins, E.L., and Addo, K.A. (2024). Misperception of drivers of risk alters willingness to adapt in the case of *Sargassum* influxes in West Africa. *Global Environmental Change 84*, 102779. https://doi.org/10.1016/j.gloenvcha.2023.102779

Zhang, C., Sun, S., He, S., and Wu, C. (2022). Direct air capture of CO_2 by KOH-activated bamboo biochar. *Journal of the Energy Institute 105*, 399-405. https://doi.org/10.1016/j.joei.2022.10.017